

ELECTRICAL ENGINEERING

Small-signal stability analysis for two-area interconnected power system with load frequency controller in coordination with FACTS and energy storage device



Ravi Shankar, Ravi Bhushan *, Kalyan Chatterjee

Department of Electrical Engineering, ISM Dhanbad, Dhanbad 826004, India

Received 5 November 2014; revised 21 June 2015; accepted 29 June 2015
Available online 15 August 2015

KEYWORDS

Small signal stability;
Eigenvalues;
Participation factor;
Redox Flow Battery (RFB);
Static Synchronous Series
Compensator (SSSC);
Load frequency control
(LFC)

Abstract This paper deals with the modelling and small signal stability analysis for the two areas interconnected power system using a load frequency controller. The eigenvalues and the participation factor analysis are used to examine the small signal stability and contribution of different states in a particular eigenvalue of the system, respectively. A load frequency controller is designed to stabilize the frequency deviations which occur due to the small perturbation in the system. In this paper, the proposed control scheme consists of an integral controller in coordination with the Redox Flow Energy Storage System (RFESS) and the Static Synchronous Series Compensator (SSSC). The dynamic responses of the overall system have been improved by the proposed controller, which is also verified with the help of eigenvalue and participation factor analysis. This analysis shows that overall system oscillation has been reduced through a proposed controller.

© 2015 Faculty of Engineering, Ain Shams University. Production and hosting by Elsevier B.V. This is an open access article under the CC BY-NC-ND license (<http://creativecommons.org/licenses/by-nc-nd/4.0/>).

1. Introduction

A healthy power system is characterized by its different system parameters and the reliable economic control strategy for its

successful operation. Load frequency control (LFC) is an important mechanism which is to be incorporated in the power system design to get the desired output. The main aim of the LFC is to keep the frequency at nominal value as well as to regulate the net tie-line power within prescribed limits. In the present scenario, conventional generating power system consists of thermal and hydro power units. Most of the literature survey [1–8] shows that the field of LFC studies for interconnected power system containing hydro and thermal units or its various combinations. The transfer function of the hydro turbine having non-minimum phase characteristic makes the hydro power plant largely different from the steam turbine power system. The gas power system has been also integrated into the grid, but they are mainly used to meet the peak load

* Corresponding author. Mobile: +91 8862950216.

E-mail addresses: ravi060173@gmail.com (R. Shankar), ravibhushaniitbhu@gmail.com (R. Bhushan), kalyanbit@yahoo.co.in (K. Chatterjee).

Peer review under responsibility of Ain Shams University.



Production and hosting by Elsevier

demand, so that the reliability of the power system can be maintained. So, it becomes very essential to study and analyze the behavior of LFC for the diverse source of the interconnected power system. In recent years, there is fast, innovative development towards the electronic switches and device, which are widely accepted for stability and control mechanism in the power system. These Devices are commonly known as FACTS (Flexible AC Transmission System) device and energy storage devices which enhances the power transfer capability and power management of the interconnected power system [10]. Some FACTS devices like Static Synchronous Series Compensator (SSSC) [8–10], Thyristor Control Phase Shifter (TCPS) and Unified Power Flow Controller (UPFC) etc., are used to improve the reliability and power transfer capability of the power system. Bhatt et al. [8] described the LFC coordinating the control scheme of SMES-TCPS and SSSC for the interconnected power system. Chatterjee et al. and Pradhan et al. has also presented their research work which involves the coordinated control methodology using SSSC and TCSC for the interconnected power system [11,12]. Subbaramaiah et al. has described the automatic generation control in coordination with SSSC and TCPS [13] for two area power system. Energy storage systems such as Capacitive Energy Storage System (CES), Redox Flow Battery (RFB) [14], and Superconducting Magnetic Energy Storage (SMES) [8,11,12] have been widely accepted for solving the load frequency control problems. Abraham et al. has proposed automatic generation control scheme considering CES for the power system [15]. In [16–19], the GA technique is presented for AGC gains of two-area interconnected power system. Panda et al. [20], Rout et al. [21] as well as Daneshfar [22], Kuntia et al. [23] presented some of their LFC techniques which involve evolutionary technique like, Genetic Algorithm (GA), PSO, etc., which act the vital role to achieve the desired output. The eigenvalues and participation factor analysis [24] is the most effective method to analyze the small signal stability of any system. This stability analysis has been incorporated into the present work of the simulated system considering with and without the effect of the proposed control methodology. If the disturbance is persisting for the longest time, then only conventional controller or above reported control methodology for LFC of the discussed literature may not be sufficient to reduce the mismatch between load demand and generation and resulting in the frequency deviation from its nominal value. The maiden attempt has been made in this paper for the LFC of multi-area power systems with co-ordination with FACTS devices and an energy storage system. Hence, the SSSC is installed in between the tie-line to regulate the tie-line power flow and RFB are placed in each area to support the LFC during load perturbation of the interconnected power system. This work deals with a suitable and efficient, coordinated integral control scheme in coordination with the SSSC and RFB for the simulated interconnected power system. The optimum gain of an integral controller is optimized through Genetic Algorithm (GA) technique. The proposed control arrangement suppresses the frequency oscillation and net tie-line power exchange effectively, which improves the LFC mechanism for the small load perturbation.

The layout of this paper is as follows: After a short introduction, the modelling of the interconnected power system is presented in Section 2. Sections 3 and 4 describe the linearized model of SSSC and Energy Storage System, respectively. The

Performance Index and optimization of LFC through the GA procedure are given in Section 5. Section 6 demonstrates the small signal stability approach of the interconnected power system. Result and discussions are given in Section 7 and paper is finally concluded in Section 8.

2. Modelling of the interconnected power system

Mathematical Modelling of two-area interconnected power system has been used where both $area_1$ and $area_2$ are assumed to be identical. These areas consist of three different generating power units, i.e. reheat thermal turbine, hydro turbine and the gas-turbine power units. The non-linearity such as Governor Dead Band and Generation Rate Constraint (GRC) are also taken into consideration because they are always present in real-time scenario and their detailed analysis is discussed in the IEEE committee report [25]. The transfer function models of both steam and hydro turbines are discussed and developed in the IEEE committee report [26]. The modelling of gas turbine and its transfer function studies have been carried out for analyzing and testing, which are based on an IEEE report [27] and Rowen work [28]. The transfer function model of the simulated power system is given in Fig. 1. The Energy Storage System (ESS) supports the secondary controller of LFC during their lag time, so dynamic performance of the system can be improved during the transient condition. Therefore, the RFESS unit has been installed in both the interconnected areas and the input signal of the RFB is the area control error of the corresponding area. The SSSC is used in the synthesis of a three-phase voltage in quadrature with the line current to emulate an inductive or capacitive reactance for influences the power flow through the transmission line for desired results. The proposed control strategy and its investigation are carried out in detail for improvement of the LFC as well as the dynamic performance of the simulated test system.

3. Linearized model of the Static Synchronous Series Compensator (SSSC) for LFC

Static Synchronous Series Compensator is installed in series with the tie-line and used as a frequency stabilizer for the interconnected power system. Equivalent circuit diagram of the SSSC with the tie-line is given in Fig. 2. The SSSC is capable of providing inductive as well as capacitive reactance to the transmission line. Hence, it can regulate and control the active power to the transmission line. The SSSC is mainly used in the transmission line to reduce the oscillation of the system. The SSSC compensation can be controlled by changing the magnitude of the injected voltage \bar{U}_s and its polarity according to the requirement. It also depends upon the transformer reactance X_s . In Fig. 3 [8,10,13], the SSSC structure consists of a proportional gain block in combination of proper phase-lead compensation characteristics to compensate the suitable phase lag between output and input signal. From Fig. 4, it is obvious that the line current (when $\bar{U}_s = 0$) is:

$$\bar{I}_0 = \left(\frac{\bar{U}_m - \bar{U}_n}{jX_T} \right) \quad (1)$$

where $X_T = X_L + X_s$ and angle of the line current is given by

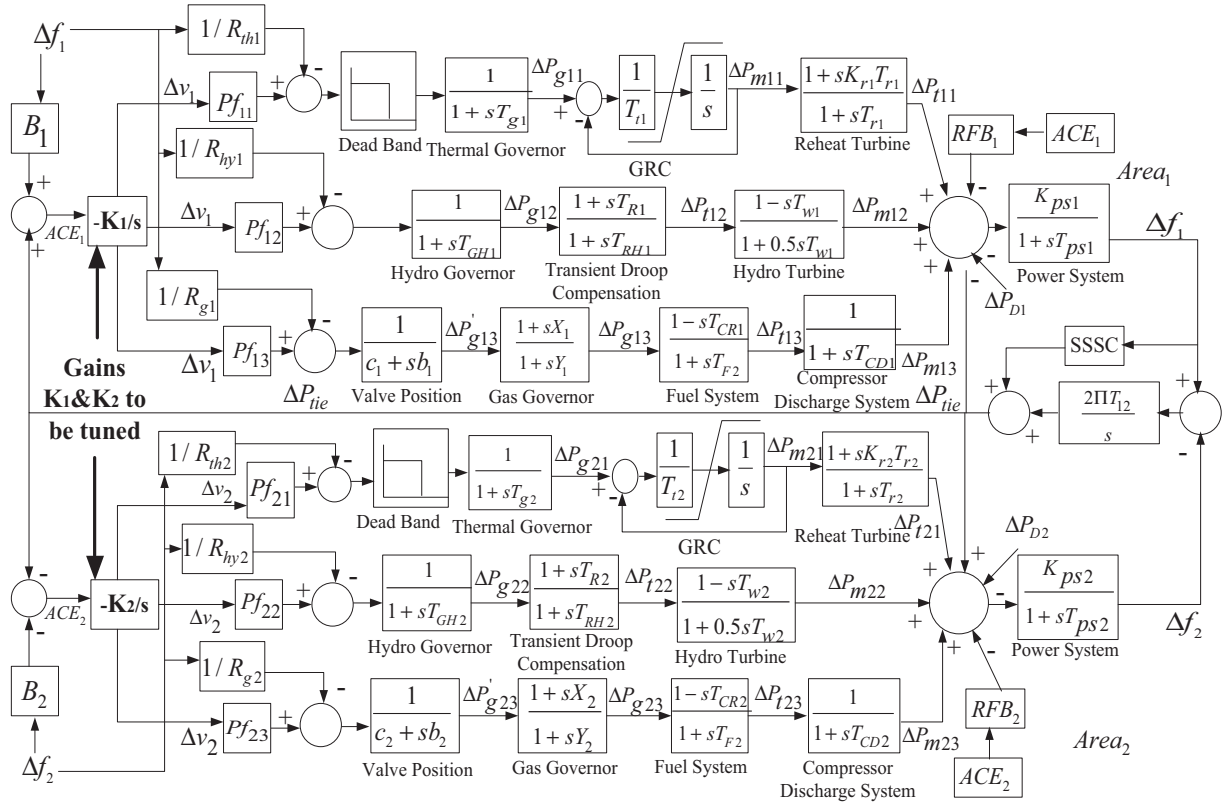


Figure 1 Reduced equivalent transfer function block diagram of multi generating interconnected power system.

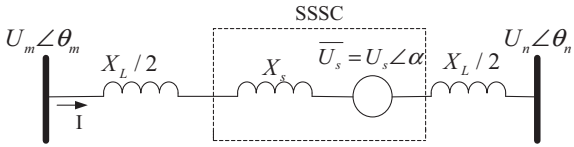


Figure 2 Equivalent circuit diagram of the SSSC with tie-line.

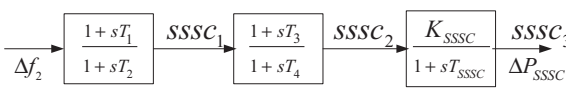


Figure 3 Block diagram of SSSC.

$$\theta_c = \tan^{-1} \left(\frac{U_n \cos \theta_n - U_m \cos \theta_m}{U_m \sin \theta_m - U_n \sin \theta_n} \right) \quad (2)$$

From Fig. 5, the line current can be written as:

$$\bar{I} = \left(\frac{\bar{U}_m - \bar{U}_s - \bar{U}_n}{jX_T} \right) = \bar{I}_0 + \bar{\Delta I} \quad (3)$$

$\bar{\Delta I}$ is an additional current due to SSSC voltage \bar{U}_s .

The power flow from m bus to n bus is given as:

$$\bar{S} = U_m \bar{I}^* = \bar{S}_{mno} + \bar{\Delta S}_{mn} \quad (4)$$

$$P_{mn} + jQ_{mn} = (P_{mno} + \Delta P_{mn}) + j(Q_{mno} + \Delta Q_{mn}) \quad (5)$$

P_{mno} and Q_{mno} are the real and reactive power flows respectively, when $\bar{U}_s = 0$.

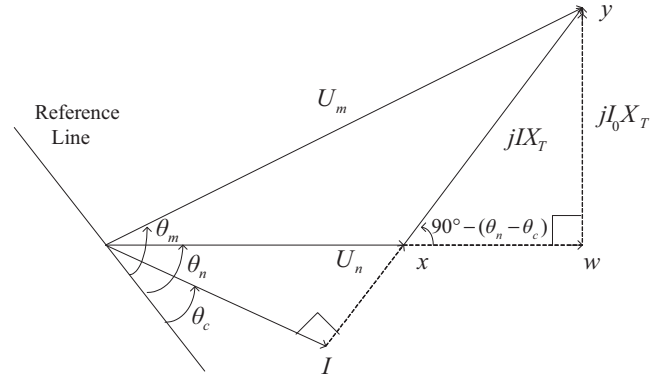


Figure 4 Phasor diagram when magnitude of injected voltage is zero.

The change in real power flow caused by the SSSC voltage \bar{U}_s is given by

$$\Delta P_{nm} = \frac{U_m U_s}{X_T} \sin(\theta_m - \alpha) \quad (6)$$

When U_s lags the current by 90° ($\alpha = \theta_c - 90^\circ$) which is shown in Fig. 5, ΔP_{nm} can be written as follows:

$$\Delta P_{nm} = \frac{U_m U_s}{X_T} \cos(\theta_m - \theta_c) \quad (7)$$

From Fig. 4, the term $\cos(\theta_m - \theta_c)$ can be written as:

$$\cos(\theta_m - \theta_c) = \frac{U_n}{U_m} \cos(\theta_n - \theta_c) \quad (8)$$

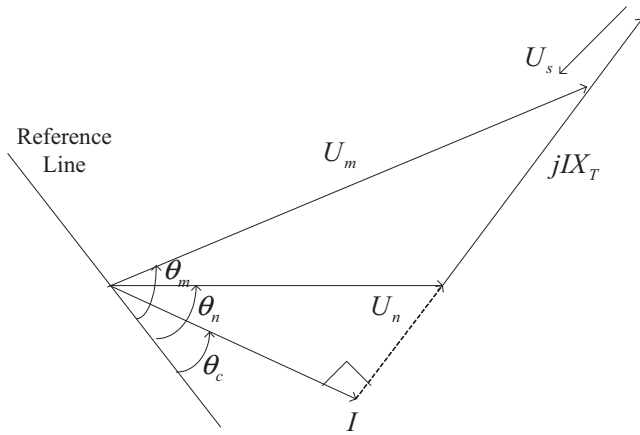


Figure 5 Phasor diagram when voltage lags the current by 90 degree.

From Fig. 4, we can be also written as:

$$\cos(\theta_n - \theta_c) = \frac{yw}{xy} \quad (9)$$

$$yw = U_m \sin(\theta_{mn}) \quad (10)$$

$$xy = \sqrt{(U_m^2 + U_n^2 - 2U_m U_n \cos \theta_{mn})} \text{ and } \theta_{mn} = (\theta_m - \theta_n) \quad (11)$$

By using the above relationship, the term ΔP_{mn} can be expressed as:

$$\Delta P_{mn} = \frac{U_m U_n}{X_T} \sin \theta_{mn} \times \left(\frac{U_s}{\sqrt{(U_m^2 + U_n^2 - 2U_m U_n \cos \theta_{mn})}} \right) \quad (12)$$

From Eq. (5), $P_{mn} = P_{mno} + \Delta P_{mn}$

$$\Delta P_{mn} = \frac{U_m U_n}{X_T} \sin \theta_{mn} + \left(\left(\frac{U_m U_n}{X_T} \sin \theta_{mn} \right) \times \left(\frac{U_s}{\sqrt{(U_m^2 + U_n^2 - 2U_m U_n \cos \theta_{mn})}} \right) \right) \quad (13)$$

By linearizing the Eq. (13) about its operating point, it can be written as:

$$\Delta P_{mn} = \frac{U_m U_n}{X_T} \cos(\theta_m - \theta_n) (\Delta \theta_m - \Delta \theta_n) + \left\{ \left(\frac{U_m U_n \sin \theta_{mn}}{X_T} \right) \times \left(\frac{\Delta U_s}{\sqrt{(U_m^2 + U_n^2 - 2U_m U_n \cos \theta_{mn})}} \right) \right\} \quad (14)$$

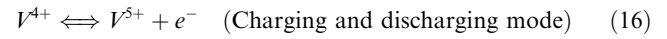
$$\Delta P_{mn} = \Delta P_{Tie-line} + \Delta P_{SSSC} \quad (15)$$

4. Modelling of the Energy Storage System for LFC

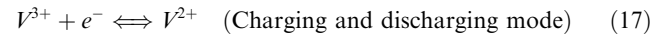
The Energy Storage System can provide the quick energy-storing action with additional to the kinetic energy of the generator which can share the sudden load change in a power system. Hence, it can eliminate the electromagnetic oscillation of the dis-

turbed power system. In this study, the RFB has been used as an energy storage device. RFB has a wide range of applications and excellent characteristic like load levelling, higher capacity than conventional battery, quick response as it takes very small time to come into operation when requires. It is also free from self-discharge problem as the electrolytes are kept in different chambers according to the availability of space and long service life as well. The RFB contains the sulfuric acid with vanadium ions, which is used as the positive and negative ion electrolytes and involved the following basic chemical reactions:

At Positive Electrodes,



At Negative Electrodes,



Due to the delayed response of the lag time of the governor and other mechanism of the system, RFB gives the quick and fast energy-storing action to the power system. Hence, due to lag time hunting does not occur during the load perturbation. This is the reason that, ACE feeds directly the controlling input signal to the RFB unit. The block diagram of Redox Flow Battery is shown in Fig. 6. The Eq. (18) shows the implementation of the RFB unit to the system [14].

$$\left\{ (ACE \times K_{rfb}) - \left(\frac{K_{ri}}{1 + sT_{ri}} \right) \right\} \left(\frac{1}{1 + sT_{di}} \right) - (setvalue) = \Delta P_{rfb} \quad (18)$$

5. Optimization of an integral controller gain through Genetic Algorithm (GA) approach

First of all, the objective function is defined for the studied system, i.e., the performance index of the system, which is the combination of the frequency deviations of both area (Δf_1 & Δf_2) and net tie-line power flow (ΔP_{tie}) of the interconnected power system. Hence, Integral Square Error (ISE) acts as an objective function for the optimization purpose of an integral controller gain of the proposed interconnected power system.

$$ISE = \int_0^t (\Delta f_1^2 + \Delta f_2^2 + \Delta P_{tie}^2) dt \quad (19)$$

Now the GA is used for getting the optimized value of the integral gains of an integral controller. With the help of genetic programming, the optimized value of the integral gains of an integral controller is obtained to achieve the desired output with the proposed load frequency control scheme. Corresponding system performance parameters like peak time, peak value, rise time, settling time and the value of performance index for ISE are obtained and shown in the Table 1. The value of the performance index is minimized and obtained the corresponding optimal value of the integral gain (K_i) of the controller for both the area and feeding it into the studied system. Binary coding is chosen to represent the problem parameters, i.e. a selection operator, a crossover operator and a mutation operator. Population size (n), Crossover probability (P_c) and mutation probability (P_m) are selected and random population of string of size (l) is initialized. As the iteration proceeded, the error is minimized i.e., value of performance index gets minimized and getting the corresponding optimal value of the integral gain (K_i) of the con-

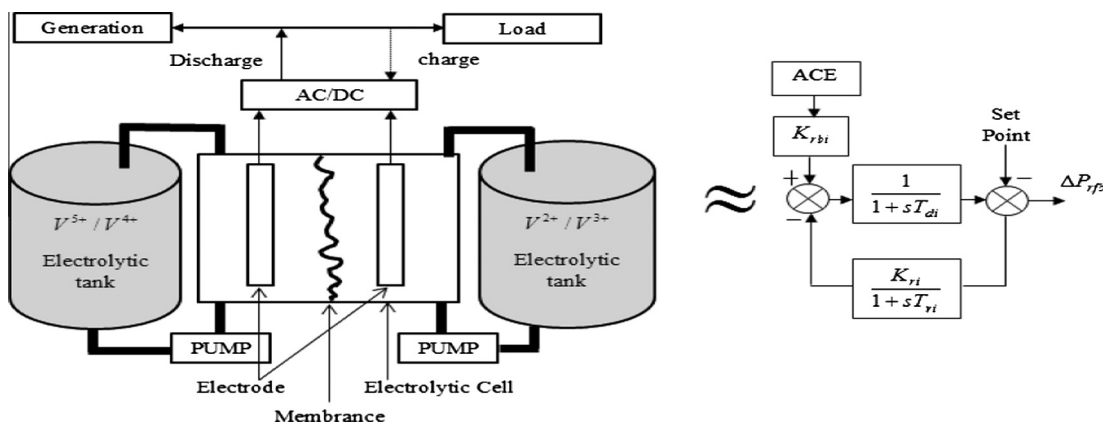


Figure 6 Block diagram of Redox Flow Battery (RFB).

Table 1 Dynamic performance characteristics of the studied system with proposed control scheme.

	With optimal control scheme [29]	With proposed controller	Percentage improvement
Value of the Integral gains of both area	–	$K_1 = 0.699$ $K_2 = 0.325$	–
Value of the performance index	–	ISE = 0.0002	–
Characteristics of the frequency deviation (Δf_1) of area 1	Peak Amplitude: 0.0327 pu RiseTime: 0.1356 s PeakTime: 1.9500 s Settling Time: 28.12 s	Peak Amplitude: 0.0053 pu Rise Time: 4.18e–04 s Peak Time: 1.781 s Settling Time: 22.03 s	83.79 99.69 8.66 21.65
Characteristics of the frequency deviation (Δf_2) of area 2	Peak Amplitude: 0.0236 pu RiseTime: 0.1142 s PeakTime: 1.8000 s Settling Time: 30.21 s	Peak Amplitude: 0.0078 pu Rise Time: 0.017 s Peak Time: 0.579 s Settling Time: 23.45 s	66.94 85.11 67.83 22.37
Characteristics of tie-line power flow deviation (ΔP_{tie}) of the interconnected power system	Peak Amplitude: 0.0070 pu RiseTime: 0.1431 s PeakTime: 1.9000 s Settling Time: 37.93 s	Peak Amplitude: 0.0028 pu Rise Time: 0.1082 s Peak Time: 0.194 s Settling Time: 37.51 s	60 24.38 89.78 1.10

troller for both area and it is fed to the simulated test system. Functional Block Diagram of Genetic Algorithm is given in Fig. 7. There are seven major steps are defined in the process of GA which is as follows:

- Step1:** A binary coding [19] is chosen to represent the problem parameters or objective functions, i.e. a selection operator, a crossover operator and a mutation operator. Chose population size ($n = 20$), Crossover probability ($P_c = 0.8$) and mutation probability ($P_m = 0.05$) are chosen. Initialized a random population of string of size ($l = 32$).
- Step2:** A maximum allowable number is chosen $t_{max} = 100$ and set $t = 0$.
- Step3:** Each string is evaluated and its fitness function for an ISE performance index of the simulated interconnected power system are calculated.
- Step4:** If $t > t_{max}$ or other termination criterion is satisfied, terminate the process otherwise proceed further for genetic operation and get the optimized value of the integral gain (K_i) of the integral controller in both areas.

- Step5:** Perform reproduction of the population on each performance indices taken as an objective function for optimization process to get the optimal value of the integral gain.
- Step6:** perform crossover of randomly selected pairs of strings having a probability of 0.8.
- Step7:** Perform Mutation on a string which is randomly selected having a lower probability than crossover.
- Step8:** Evaluate string in the new population, set $t = t + 1$ and go to step 4.

6. Small signal stability analysis of the interconnected power system

The linearized state-space representation is as follows:

$$\dot{X} = AX + BV \tag{20}$$

$$Y = CX \tag{21}$$

$$|\lambda I - A| = 0 \tag{22}$$

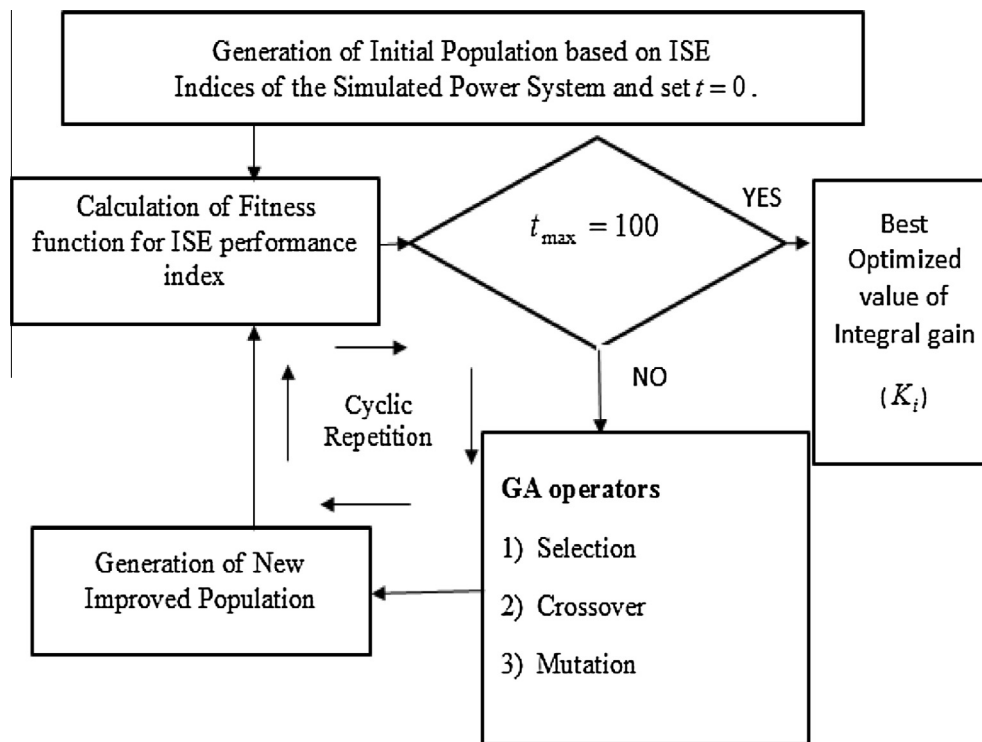


Figure 7 Functional block diagram of Genetic Algorithm (GA).

where $X = [X_1, X_2, \dots, X_N]^T$ is the state vector, N is the number of state variables, $V = [V_1, V_2, \dots, V_M]^T$ is the input (or control) vector, M is the number of control variables, $Y = [Y_1, Y_2, \dots, Y_P]^T$ is the output vector, P is the number of output variables and A, B, C are a constant matrix with dimensions of $N \times N, N \times M$ and $P \times N$ respectively.

λ = eigenvalues of the system.

The 25 state variables of the studied system for without proposing controller are:

$$X = \left[\begin{array}{l} \Delta f_1, \Delta f_2, \Delta P_{tie}, \Delta P_{m21}, \Delta P_{g22}, \Delta P_{t22}, \Delta P_{m22}, \Delta P_{m23}, \Delta P_{m11}, \Delta P_{g12}, \Delta P_{t12}, \Delta P_{m12}, \Delta P_{m13}, \Delta v_2, \Delta v_1, \\ \Delta P_{g11}, \Delta P_{t11}, \Delta P_{g21}, \Delta P_{t21}, \Delta P'_{g13}, \Delta P_{g13}, \Delta P'_{g23}, \Delta P_{g23}, \Delta P_{t23}, \Delta P_{t13} \end{array} \right]^T$$

And the 28 state variables of the studied system for proposed controller are:

$$X = \left[\begin{array}{l} \Delta f_1, \Delta f_2, sssc1, \Delta P_{tie}, \Delta P_{m21}, \Delta P_{g22}, \Delta P_{t22}, \Delta P_{m22}, \Delta P_{m23}, \Delta P_{m11}, \Delta P_{g12}, \Delta P_{t12}, \Delta P_{m12}, \Delta P_{m13}, \Delta v_1, \\ \Delta v_2, sssc3, sssc2, \Delta P_{g11}, \Delta P_{t11}, \Delta P_{g21}, \Delta P_{t21}, \Delta P'_{g13}, \Delta P_{g13}, \Delta P'_{g23}, \Delta P_{g23}, \Delta P_{t23}, \Delta P_{t13} \end{array} \right]^T$$

In this paper, the small signal stability analysis is described in two different cases. Case (A) deals with the stability analysis only with integral controller and case (B) associated with the stability analysis considering the proposed load frequency con-

troller. In both cases, the stability analysis is based on the eigenvalue and the participation factor method. The results associated with these cases are given in the result and discussion section.

7. Results and discussion of the simulated test system

The simulation of proposed controller is carried out using the MATLAB/Simulation Toolbox. To simplify the analysis, both of the interconnected areas are assumed to be identical.

All the parameters of the studied system have been given in Appendix A. As mentioned in Section 5, the Genetic Algorithms (GA) has been successfully applied to tune the integral controller through the ISE performance index. All the

analysis has been done at the load change of 0.01 pu in both the areas and the results of the small signal stability in the case of with and without proposed controller is given as follows:

Case (A): Small signal stability analysis without proposed controller

In the proposed study system, the total number of state variables is twenty-five. With the help of a state-space approach, system matrix of the studied system has been generated and the time domain response characteristics of the studied system are obtained which is shown in Table 1. The eigenvalues and the corresponding damping factor, damping frequency and dominant states are given in Table 2.

Case (B): Small signal stability analysis with proposed controller

In this case, the integral controller with the FACTS device (SSSC) and the RFB is incorporated for load frequency control of the interconnected power system. The integral controller gains K_1 and K_2 of the both areas have been tuned only for a particular load change. The proposed controller has been improved the dynamic responses of the overall system which are given in the Table 1. The total number of state variables is increased twenty-five to twenty-eight for this proposed controller and the eigenvalues and the corresponding damping factor, damped frequency and dominant states are given in Table 2.

Table 1 show the optimized value of the integral controller gains of $area_1$ and $area_2$ are 0.6999 and 0.3250, respectively, and the corresponding minimized value of the ISE performance index is 0.0002. The time domain characteristics of the frequency deviation of $area_1$, $area_2$ and the tie-line power flow deviation and the corresponding percentage improvement are also given in Table 1. To show the effectiveness of the proposed control methodology, it has been compared with the optimal control scheme [29].

With the help of above optimized integral gains, a new system matrix is constructed and then the eigenvalues and the participation factors of the proposed system is evaluated. The damping factors and damped frequencies are calculated with the help of eigenvalues of the system, whereas the dominant states are decided by the participation factors of the studied system. The largest value of the participation factor indicates the maximum contribution of the state variables in a particular eigenvalue. The participation factors look at the normalized contribution of various dynamic states on the damping of the specific mode of the system. The mathematical formulation concept of participation factor has been taken from reference number [1] (page 708 to 716).

Participation factor analysis shows that the contribution of dominant states which are caused for the oscillations in the case of with and without proposed control scheme with respect to their eigenvalues. From the results given in Table 2, it has

Table 2 Results of the studied system with and without proposed control scheme.

State variables	Without proposed control scheme				With proposed control scheme			
	Eigenvalues	Damp factor	Damp Freq (Hz)	Dominant states	Eigenvalues	Damp factor	Damp Freq (Hz)	Dominant states
Δf_1	$-19.83(\lambda_1)$	1	0	ΔP_{g13}	$-71.57(\lambda_1)$	1	0	ΔP_{g11}
Δf_2	$-19.84(\lambda_2)$	1	0	ΔP_{g23}	$-14.14 + 15.71i(\lambda_2)$	0.67	2.5	$\Delta f_1, sssc1, \Delta P_{g11}, sssc3$
ΔP_{tie}	$-12.79(\lambda_3)$	1	0	ΔP_{g11}	$-20.12(\lambda_4)$	1	0	ΔP_{g13}
ΔP_{m21}	$-12.78(\lambda_4)$	1	0	ΔP_{g21}	$-19.78(\lambda_5)$	1	0	ΔP_{g23}
ΔP_{g22}	$-7.07(\lambda_5)$	1	0	$\Delta P_{m13}, \Delta P_{r13}$	$-12.96(\lambda_6)$	1	0	ΔP_{r13}
ΔP_{r22}	$-6.99(\lambda_6)$	1	0	$\Delta P_{m23}, \Delta P_{r23}$	$-12.29(\lambda_7)$	1	0	ΔP_{r11}
ΔP_{m22}	$-0.09 + 2.79i(\lambda_7)$	0.03	0.45	$\Delta f_1, \Delta f_2, \Delta P_{tie}$	$-8.06(\lambda_8)$	1	0	$\Delta f_2, \Delta P_{m11}, \Delta P_{g23}$
ΔP_{m23}	$-0.09 - 2.79i(\lambda_8)$	0.03	0.45	$\Delta f_1, \Delta f_2, \Delta P_{tie}$	$-4.67 + 1.79i(\lambda_9)$	0.93	0.29	$\Delta v_1, sssc3, \Delta P_{g11}, \Delta P_{g13}$
ΔP_{m11}	$-0.36 + 2.18i(\lambda_9)$	0.16	0.35	$\Delta f_1, \Delta f_2$	$-4.67 - 1.79i(\lambda_{10})$	0.93	0.29	$\Delta v_1, sssc3, \Delta P_{g11}, \Delta P_{g13}$
ΔP_{g12}	$-0.36 - 2.18i(\lambda_{10})$	0.16	0.35	$\Delta f_1, \Delta f_2$	$-2.59 + 2.81i(\lambda_{11})$	0.68	0.45	$\Delta f_2, \Delta P_{m11}, \Delta P_{g23}$
ΔP_{r12}	$-3.49(\lambda_{11})$	1	0	$\Delta P_{m21}, \Delta P_{m11}$	$-2.59 - 2.81i(\lambda_{12})$	0.68	0.45	$\Delta f_2, \Delta P_{m11}, \Delta P_{g23}$
ΔP_{m12}	$-3.49(\lambda_{12})$	1	0	$\Delta P_{m21}, \Delta P_{m11}$	$-4.05(\lambda_{13})$	1	0	sssc3
ΔP_{m13}	$-2.37 + 0.58i(\lambda_{13})$	0.97	0.091	$\Delta P_{g22}, \Delta P_{m22}$	$-3.46(\lambda_{14})$	1	0	ΔP_{m21}
Δv_2	$-2.37 - 0.58i(\lambda_{14})$	0.97	0.091	$\Delta P_{g22}, \Delta P_{m22}$	$-2.06 + 0.52i(\lambda_{16})$	0.97	0.08	$\Delta P_{r22}, \Delta P_{m23}$
Δv_1	$-2.31 + 0.62i(\lambda_{15})$	0.97	0.098	$\Delta P_{g12}, \Delta P_{m12}$	$-3.39(\lambda_{15})$	1	0	ΔP_{g12}
ΔP_{g11}	$-2.31 - 0.62i(\lambda_{16})$	0.97	0.098	$\Delta P_{g12}, \Delta P_{m12}$	$-2.0 - 0.29i(\lambda_{19})$	0.99	0.05	$\Delta P_{r12}, \Delta P_{m13}$
ΔP_{r11}	$-1.44(\lambda_{17})$	1	0	$\Delta P_{m22}, \Delta P_{g23}$	$-1.21(\lambda_{20})$	1	0	$\Delta P_{r21}, \Delta P_{r23}$
ΔP_{g21}	$-1.36(\lambda_{18})$	1	0	$\Delta P_{g23}, \Delta P_{g13}$	$-1.14(\lambda_{21})$	1	0	$\Delta P_{r21}, \Delta P_{r23}$
ΔP_{r21}	$-0.45 + 0.27i(\lambda_{19})$	0.85	0.04	$\Delta P_{tie}, \Delta v_2$	$-0.43(\lambda_{22})$	1	0	ΔP_{tie}
$\Delta P'_{g13}$	$-0.45 - 0.27i(\lambda_{20})$	0.85	0.04	$\Delta P_{tie}, \Delta v_2$	$-0.09 + 0.09i(\lambda_{23})$	0.66	0.02	$\Delta v_2, \Delta P_{g21}$
$\Delta P'_{g13}$	$-0.13 + 0.06i(\lambda_{21})$	0.92	0.01	$\Delta v_1, \Delta P_{r11}$	$-0.09 - 0.09i(\lambda_{24})$	0.66	0.02	$\Delta v_2, \Delta P_{g21}$
$\Delta P'_{g23}$	$-0.13 - 0.06i(\lambda_{22})$	0.92	0.01	$\Delta v_1, \Delta P_{r11}$	$-0.07 + 0.06i(\lambda_{25})$	0.79	0.01	$\Delta P_{g22}, sssc2$
ΔP_{g23}	$-0.15(\lambda_{23})$	1	0	ΔP_{r21}	$-0.07 - 0.06i(\lambda_{26})$	0.79	0.01	$\Delta P_{g22}, sssc2$
ΔP_{r23}	$-0.018(\lambda_{24})$	1	0	ΔP_{r12}	$-0.017(\lambda_{27})$	1	0	ΔP_{m12}
ΔP_{r13}	$-0.019(\lambda_{25})$	1	0	ΔP_{r22}	$-0.018(\lambda_{28})$	1	0	ΔP_{m22}
sssc1					$-14.14 - 15.71i(\lambda_3)$	0.67	2.5	$\Delta f_1, sssc1, \Delta P_{g11}, sssc3$
sssc2					$-2.0 + 0.29i(\lambda_{18})$	0.99	0.05	$\Delta P_{r12}, \Delta P_{m13}$
sssc3					$-2.06 - 0.52i(\lambda_{17})$	0.97	0.08	$\Delta P_{r22}, \Delta P_{m23}$

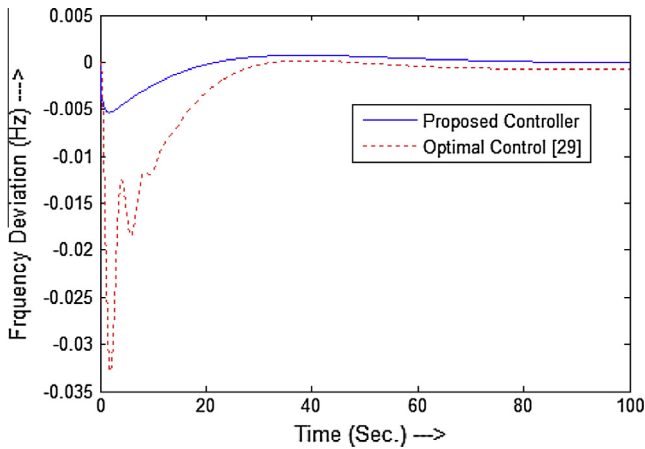


Figure 8 Frequency deviation graph of the first control area subjected to load change of 0.01 pu with their comparison for proposed control scheme and with optimal control scheme [29].

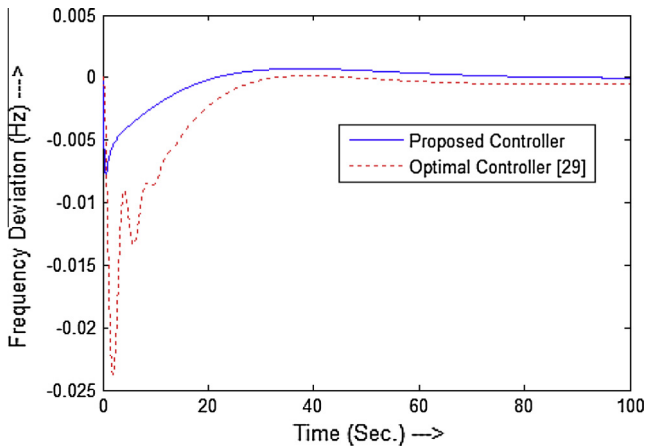


Figure 9 Frequency deviation graph of the second control area subjected to load change of 0.01 pu with their comparison of proposed control scheme and with optimal control scheme [29].

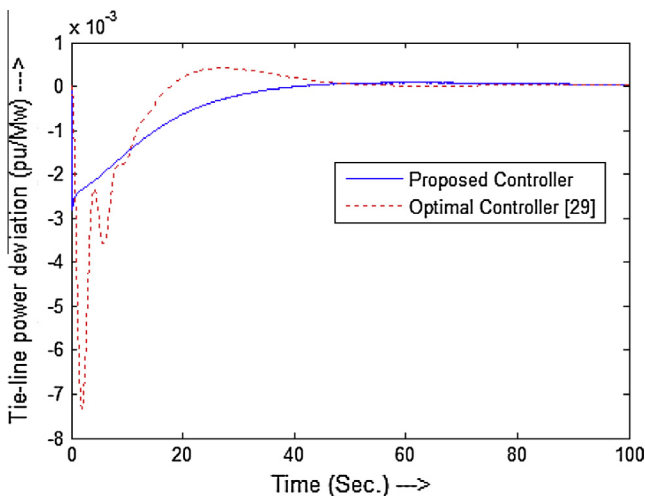


Figure 10 Tie-line power flow deviation graph of the interconnected power system subjected to load change of 0.01 pu and their comparison for proposed control scheme & with optimal control scheme [29].

been observed that in the case of proposed controller, most of the eigenvalues have much more negative real part compared to without controller, so the stability of the overall system has improved. The behavior of frequency and tie-line power are more important to study the small signal stability problem of this system. When the proposed controller is used in the system, the stability and damping of frequency as well as tie-line power are enhanced and the corresponding plots are presented in Figs. 8–10. These figures are also represented the comparison of the frequency deviation of $area_1$ and $area_2$ of the proposed control scheme and with the optimal control scheme [29]. From the simulation results, it can be seen that the proposed control scheme works efficiently for the simulated interconnected power system, which ensures better, effective and improved dynamic response over the optimal control scheme.

8. Conclusion

This paper describes the small signal stability analysis of the interconnected power system when the load frequency integral controller incorporated with the FACTS and Energy Storage device. The stability analysis has been done with the help of eigenvalues and the participation factor method. The analysis shows that in the case of the proposed control scheme the number of oscillating mode is reduced and it has been also verified graphically by the results obtained from the simulation studies. All the dynamic and transient response parameters evolution is based upon an ISE performance index of the interconnected power system and the gain of the integral controller is optimized through Genetic Algorithm (GA) technique. The above control technique is very efficient for LFC, which shows the improved dynamic performance and small signal stability with the variation of 0.01 pu step load change.

Appendix A. Parameters of the studied system

A.1. Thermal power system

Coefficients of re-heat steam turbine = $K_{r1} = K_{r2} = 0.3$, Re-heat time constants = $T_{r1} = T_{r2} = 10$ s, Turbine time constants = $T_{t1} = T_{t2} = 0.3$ s, R_{th} Speed governor regulations = $R_{th1} = R_{th2} = 2.4$ Hz/puMW, Speed governor time constants = $T_{g1} = T_{g2} = 0.8$ s and Water time constants = $T_{w1} = T_{w2} = 1$ s, GRC = 0.0017 pu, Dead band = 0.006 pu.

A.2. Gas power system

Speed governor lead time constants = $X_1 = X_2 = 0.6$ s, Speed governor lag time constants = $Y_1 = Y_2 = 1$ s, Valve positional constants ($a_1 = a_2 = 1$, $b_1 = b_2 = 0.05$ & $c_1 = c_2 = 1$), Fuel time constants = $T_{F1} = T_{F2} = 0.23$ s, T_{CR} . Combustion reaction time delays = $T_{CR1} = T_{CR2} = 0.3$ s, Compressor discharge volume time constant = $T_{CD1} = T_{CD2} = 0.2$ s and Speed governor regulation = $R_{G1} = R_{G2} = 2.4$ Hz/puMW.

A.3. Hydropower system

Speed governor rest time = $T_{R1} = T_{R2} = 5$ s, Transient droop time constants = $T_{RH1} = T_{RH2} = 28.75$ s, Main servo time con-

stant = $T_{GH1} = T_{GH2} = 0.2$ s, and Speed governor regulation = $R_{hy1} = R_{hy2} = 2.4$ Hz/puMW.

A.4. Power system

Gain of the power systems = $K_{PS1} = K_{PS2} = 120$ Hz/pu, Time constants of the power system = $T_{PS1} = T_{PS2} = 20$ s. Participation factors representing economic load dispatch ($pf_{11} = pf_{21} = 0.46966$, $pf_{12} = pf_{22} = 0.37814$, $pf_{13} = pf_{23} = 0.15220$), Bias factor = $B_1 = B_2 = 0.425$ puMW/Hz. Integral gains of the controller ($K_1 = 0.6999$ & $K_2 = 0.325$).

A.5. RFB

$K_{ri} = 1$, $T_{di} = 0$, $T_{ri} = 0.78$, Gain of the Redox Flow Battery = $K_{rfb} = 1.8$.

A.6. SSSC

$T_1 = 0.2587$ s, $T_2 = 0.2481$ s, $T_3 = 0.2333$ s, $T_4 = 0.060$ s, Gain of SSSC = $K_{sssc} = 0.2035$, Time constant of SSSC (T_{sssc}) = 0.03 s.

References

- [1] Kundur P. Power system stability and control. New York: McGraw Hill; 1994.
- [2] Tripathy SC, Chandramohan Nair PS, Rao ND. Adaptive Automatic generation control with superconducting magnetic energy storage in power systems. IEEE Trans Energy Convers 1992;434–41.
- [3] Shiroei Mojtaba, Ranjbar Ali Mohammad, Amraee Toraj. A functional model predictive control approach for power system load frequency control considering generation rate constraint. Int Trans Electric Energy Syst 2013(23):214–29.
- [4] Kassem Ahmed M. Neural predictive controller of a two-area load frequency control for interconnected power system. Ain Shams Eng J (Elsevier) 2010;1:49–58.
- [5] Aditya. Design of load frequency controller using genetic algorithm for two areas interconnected power system. Int J Electric Power Compon Syst 2003;31:81–94.
- [6] Taher Seyed Abbas, Fini Masoud Hajiakbari, Aliabadi Saber Falahati. Fractional order PID controller design for LFC in electric power systems using an imperialist competitive algorithm. Ain Shams Eng J (Elsevier) 2014;5:121–35.
- [7] Chatterjee K. PI controller for automatic generation control based on performance indices. Int J World Acad Sci, Eng Technol 2011;75:321–8.
- [8] Bhatt Praghnes, Roy Ranjit, Ghosal SP. Comparative performance evaluation of SMES-SMES, TCPS-SMES & SSSC-SMES controllers in AGC for a two-area hydro-hydro system. Int J Electric Power Energy Syst 2011;33:1585–97.
- [9] Ngamroo I, Kongprawechnon W. A robust controller design of SSSC for stabilization of frequency oscillation in the interconnected power system. Electric Power Syst Res 2003;67:161–76.
- [10] Hingorani NG, Gyugyi L. Understanding FACTS: concepts & technology of FACTS. New York: IEEE Press; 2000.
- [11] Chatterjee K, Shankar R, Chatterjee TK. SMES coordinated SSSC of an interconnected thermal power system for load frequency control. In: Asia-Pacific Power & Energy engineering Conference (APPEEC-2012), Shanghai, China, IEEE Proc. 27–29 March, 2012, pp. 1–4.
- [12] Padhan Saroj, Sahu Rabindra Kumar, Panda Sidhartha. Automatic generation control with thyristor controlled series compensator including superconducting magnetic energy storage units. Ain Shams Eng J (Elsevier) 2014;5:759–74.
- [13] Subbaramaiah K. Improvement of dynamic performance of SSSC and TCPS based hydrothermal system under deregulated scenario employing PSO based dual mode controller. Eur J Sci Res 2011;57(2):230–43.
- [14] Chidambaram IA, Parasmasivam B. Control performance standards based load frequency controller coordinating redox flow batteries coordinate with interline power flow controller. J Power Sources 2012;219:292–304.
- [15] Abraham Rajesh Joseph, Das D, Patra Amit. Automatic generation control of an interconnected power system with capacitive energy storage. Int J Electric Electron Eng 2010;3:351–6.
- [16] Ibraheem, Singh Omveer, Hassan Namuil. Genetic algorithms based scheme for optimization of AGC gains of the interconnected power system. J Theoret Appl Inform Technol 2010;12.
- [17] Bhatt P, Roy R, Ghoshal SP. GA/particle swarm intelligence based optimization of two specific varieties of controller devices applied to two-area multi-units automatic generation control. Int J Electric Power Energy Syst 2010;32:299–310.
- [18] Shankar Ravi, Chatterjee K, Chatterjee TK. Coordination of economic load dispatch and load frequency control for interconnected power system. J Instit Eng Series-B 2015;96(1):47–54. <http://dx.doi.org/10.1007/s40031-014-0113-0>.
- [19] Deb Kalyanmoy. In: Optimization for engineering design: algorithms and examples. New Delhi: Printice Hall of India Pvt. Ltd.; 2005. p. 301–12.
- [20] Panda S, Yegireddy NK. Automatic generation control of multi area power system using multi objective non-dominated sorting GA-II. Electric Power Energy Syst 2013;53:54–63.
- [21] Rout UK, Sahu RK, Panada S. Design and analysis of differential evolution algorithm based AGC for the interconnected power system. Ain Shams Eng J 2013;4:409–21.
- [22] Daneshfar F, Bevarani H. Multi objective design of load frequency control using GA. Electric Power Energy Syst 2012;42:257–63.
- [23] Kuntia SR, Panda S. Simulation study for automatic generation control of a multi area power system by ANFIS approach. Appl Soft Comput 2012;12:333–41.
- [24] Du Wenjuan, Wang Haifeng, Cai Hui. Modelling a grid-connected SOFC power plant into power systems for small-signal stability analysis and control. Int Trans Electric Energy Syst 2013;23:330–41.
- [25] IEEE Working Group Report, Dynamic models of fossil fuelled steam units in power system studies, IEEE Transaction on Power Systems 6, 1991, pp. 753–61.
- [26] IEEE Committee Report, Dynamic model for steam & hydro turbines in power system studies, IEEE Transactions on Power Apparatus & System PAS-92, 1973, pp. 1904–15.
- [27] Pourbek P. Modeling of combined cycle power plant for power system studies. IEEE Power Eng Soc Gen Meet 2003;3:1308–13.
- [28] Rowen WI. Simplified mathematical representation of heavy duty gas turbine. Trans ASME J Eng Power 1983;105:865–70.
- [29] Parmar KPS, Majhi S, Kothari DP. Improvement of dynamic performance of LFC of the two area power system. Int J Comput Appl 2012;40:28–32.



Ravi Shankar received his B.Tech degree in Electrical Engineering from BIT Sindri, Dhanbad, India. He completed the Ph.D. degree in Power System, January 2015 from Indian School of Mines (ISM) Dhanbad, Jharkhand and currently working as an Assistant Professor, School of Electrical Engineering, KIIT University, Bhubaneswar, India.



Ravi Bhushan received his B.Sc. Engineering degree in Electrical Engineering, in 2009 from the Bhagalpur College of Engineering, Bhagalpur, India. He received the M.Tech. degree in Power System, in 2011 from IIT BHU, Varanasi, India. In July 2011, He joined the Department of Electrical Engineering, Sharda Group of Institutions, as an Assistant Professor. He is currently a Junior Research Fellow & pursuing the Ph.D. degree in Power System at Indian School of Mines, Dhanbad, India. He is also a student member of IEEE. His current research

interests include power system stability and control and Doubly Fed Induction Generator (DFIG) based Wind farms.



Kalyan Chatterjee received his M.E and Ph.D from Jadavpur University and Birla Institute of Technology (Deemed University) Ranchi, India in 1999 and 2005, respectively. He has been with the Department of Electrical Engineering, India School of Mines (ISM), Dhanbad, India where currently is an Associate professor is. Dr. Chatterjee has about 16 years of teaching and research experience. His research interests include Soft Computing techniques application in Power system, renewable power generation and power system control.